Rigorous positioning with side-looking radar imagery based on Range-Coplanarity model

CHENG Chunquan, ZHANG Jixian

Chinese Academy of Surveying and Mapping, *Beijing* 100039, *China*

Abstract: There still has some deficiencies in photogrammetric application with the existing geometric imaging model of radar imagery. In view of this situation the theoretical analysis was made firstly in this paper. Then several equations were constructed in turn, including Range-Coplanar (R-Cp) equation with explicit function form of image point coordinate, Range-Coplanarity equation in geocentric coordinate system and rigorous positioning model based on R-Cp equation. At last some tests including rigorous positioning were done with spaceborne TerraSAR-X imagery and sparse ground control point. The theory and experiments show that the proposed R-Cp model embody the attributes of image measurement coordinate as photogrammetric observation value, which make it easy to absorb and utilize mature digital photogrammetric theory and methods developed on collinear equation model for optical remote sensing images. For data processing of radar imagery photogrammetry the model can overcome the shortcomings existed in other model and improve the rigor, stability, reliability and efficiency.

Key words: Range-Coplanarity (R-Cp) equation, side-looking radar, rigorous positioning, sparse control point, exterior orientation elements, combined adjustment

CLC number: P237 **Document code:** A

Citation format: Cheng C Q and Zhang J X. 2012. Rigorous positioning with side-looking radar imagery based on Range-Coplanarity model. Journal of Remote Sensing, 16(5): 881–894

1 INTRODUCTION

Digital photogrammetry for the remote sensing imagery usually begins the work with geometric imaging model. At present, there are two kinds of rigorous geometric imaging equations for radar imagery. One is based on sensor state vector and doppler parameters, the other is based on sensor state vector and attitude parameters (exterior orientation elements). For the first kind, the leber l F and the R-D model are in the most widely used geometric models (Leberl, 1978, 1990; Johnsen, 1995), while for the second type R-Cp equation is one of simple and rigorous which is constructed by range condition and the beam center co-planarity condition (Cheng, et al., 2012) besides the radar collinear equation (Konecny & Schuhr, 1988; You, 2007).

There are several models and algorithms for SAR signal imaging including R-D, C-S, ω-K etc. (Cumming & Wong, 2005). The different deformation of SAR imagery can be caused by different motion compensation, different parameters for signal imaging or different accuracy of parameter estimation. So for SAR imagery different geometric imaging model could be rightly used only under certain conditions, and no rigorous geometric imaging model can be applied to any SAR imagery. Geometric model R-D can be apply to SAR images by R-D imaging, and R-Cp equation is applicable to the real aperture radar images or the SAR imagery which has the same imaging geometry relationship with the equivalent real aperture radar imagery (the equivalent real-aperture radar imagery got with the same or equivalent imaging parameters under the condition of the SAR sensor moving along the compensated path).

In the past years radar imagery geometry has been widely studied, and people have got idea SAR image positioning accuracy. But stable and reliable photogrammetry theories and methods still are important research contents and goals for radar imagery in the next several years. Two basic contents of traditional photogrammetry are involved in rigorous positioning processing for the remote sensing imagery. One is geometric imaging model, and the other is data adjustment processing. With simple and rigorous equation forms, R-D and the R-Cp models can both meet the basic requirement for geometric imaging equation of remote sensing imagery. But compared with co-linearity equation model for optical remote sensing imagery, there still are some deficiencies during adjustment processing for the fact that image point coordinate parameters are hidden in the two imaging equations.

(1) The positioning error of the image point has a close relation to orientation residual which is the difference between the meas-

Received: 2012-01-05; **Accepted:** 2012-04-06

Foundation: Natural Science Foundation of China (No.41071237); National High Technology Research and Development Program of China (863 program) (No.2011AA120401, No.2011AA120402)

First author biography: CHENG Chunquan (1972—), male, Ph.D., associate professor. His research interest is digital photogrammetry of optical and SAR images. E-mail: cspring@casm.ac.cn

ured image coordinate and the theoretical value calculated by orientation parameters. So the point measuring coordinate is often taken as the basic unit of the photogrammetric observed value by rigorous adjustment methods (such as bundle adjustment), and then the orientation parameters are solved with the least square sum of image point orientation residuals ($\min\sum(v_x^2+v_y^2)$) as the goal (Wang, 1971). For R-D and R-Cp equations, the y coordinate is hidden in the equation and no parameter represents the x coordinate directly. The error equation (generally referred as error equation of virtual observations), which is based on range equation, doppler equation or co-planarity equation condition, is not the one for image coordinates x, y. The unknown orientation parameters in the error equation are solved with the least square sum of the virtual observation residuals v_R, v_{fD}, v_{Cp} as the condition, which cannot ensure there is a minimum square sum of the image point coordinate residuals.

(2) The photogrammetric observed value is the image point coordinates measured by manual or image matching, and the combined adjustment between photogrammetric observed value and other observed value is a basic method to realize rigorous positioning of remote sensing image with sparse control points (Yuan, 2001; Shan, 2002). The weights of multi-source observed values play important roles to improve the stability, reliability and accuracy during the solving unknown parameters of combined adjustment (Tao, 2001). There is a close relationship between the weight and the accuracy for observed value, but the error equation of R-D or R-Cp does not build for actual observation and there is no direct "accuracy" information from virtual observation. So it brings inconvenience to the combined processing of multisource observation data which even affects the rigor and precision of data processing.

(3) In the positioning application based on R-D and the R-Cp equations, error equations are established according to geometric imaging equation conditions and there are no correction parameters v_x, v_y for image point coordinates. That means the orientation residual of each image point cannot be calculated directly by error equations. There are many matching points in the block images. The traditional method to get the orientation residuals of image points usually includes two steps: the first is to calculate the theoretical image coordinates according to orientation parameters and ground point coordinates by iteration, and then get the difference of image coordinates between the measurement values and the calculated values. If the traditional method is used to solve the orientation residuals the operating efficiency would be low obviously. Generally there is a larger measurement error from radar imagery than that of optical imagery, and gross errors not only decrease the positioning accuracy but also bring interference to the traditional posterior variance weighting methods. So detecting and removing gross errors are important steps for image positioning, while it is inconvenient to detect the gross error of radar image points with the existing geometric imaging models.

For R-Cp equation takes exterior orientation elements as its orientation parameters. So only if the model is improved to an explicit function form of image point coordinates, the mature digital photogrammetric data processing methods developed based on co-linearity equation model would be absorbed and well utilized. In this paper, the geometric imaging equation for side-looking radar imagery as Eq. (1) will firstly be constructed based on R-Cp equation. Then a stable, reliable and efficient rigorous positioning model for side-looking radar imagery will also be established.

$$(x,y)=f_{xy}(Xs,Ys,Zs,\varphi,k,X,Y,Z) \tag{1}$$

where (x, y) are image point coordinate; (X, Y, Z) are ground point coordinate; (Xs, Ys, Zs) are space coordinate of the sensor antenna; (φ, k) are pitch angle and yaw angle of attitude.

2 THE RANGE-COPLANARITY EQUATION WITH EXPLICIT FUNCTION FORM OF IMAGE POINT COORDINATE

Range-coplanar conditions refer to all the ground points corresponding to the images in the same image range line are within the radar beam center plane. The beam center plane is determined by both state vector and attitude of the sensor. Here the euclidean distance from sensor to ground target point is equal to the range measured by radar wave. The Range-Coplanarity equation is established as following (Cheng, et al., 2012)

$$\begin{cases} R=|\overrightarrow{\boldsymbol{OP}}-\overrightarrow{\boldsymbol{OS}}| \\ \vec{\boldsymbol{i}}\cdot(\overrightarrow{\boldsymbol{OP}}-\overrightarrow{\boldsymbol{OS}})=0 \end{cases} \tag{2}$$

where $\vec{\boldsymbol{i}}$ is the normal vector of beam center plane; $\overrightarrow{\boldsymbol{OP}}$ is the ground point position vector; $\overrightarrow{\boldsymbol{OS}}$ is the sensor position vector; R is measurement slant range of the radar wave. The expansion formula of Range-Coplanarity equation for φ-k-ω attitude rotating sequence is:

$$\begin{cases} (X-Xs)(\cos\varphi\cos k)+(Y-Ys)\sin k- \\ (Z-Zs)(\sin\varphi\cos k)=0 \\ (X-Xs)^2+(Y-Ys)^2+(Z-Zs)^2-(yM_r+R_0)^2=0 \end{cases} \tag{3}$$

where M_r is the slant range resolution; R_0 is nearest slant range; y is the column coordinate of the pixel in the image. y coordinate included in range equation and can be converted to an explicit function form of y easily. That is:

$$y=\left[\sqrt{(X-Xs)^2+(Y-Ys)^2+(Z-Zs)^2}-R_0\right]\Big/M_r \tag{4}$$

Side-looking radar and optical linear array imagery both belong to multi-station projection which makes push-broom imaging with moving of the sensor. Collinear equation of optical linear array imagery can be thought of as two plane equations. The beam center plane of radar imaging is similar to the plane of optical imaging which is vertical velocity direction (*SAB* plane in Fig. 1). With another plane(*SCD* plane) equation and another range equation, collinearity equation for optical imagery and range-coplanarity equa-

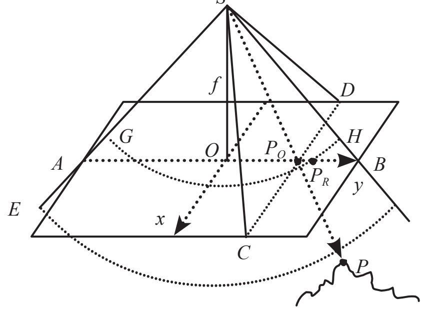

Fig. 1 Connections and differences between the Range-Coplanarity equation and collinear equation

tion for side-looking radar imagery were established respectively as shown in Fig. 1. According to collinear equation, the imaging point of the ground target point P is on the line SP_O intersected by the two planes. It can also be considered according to R-Cp equation that the imaging point is on the circular $GP_R H$ intersected by the plane and the sphere.

There is no parameter x in R-Cp model. According to the coplanarity equation the conditional equation can be established as

$$F_C = \vec{i} \cdot (\overrightarrow{OP} - \overrightarrow{OS}) = 0 \tag{5}$$

Let the image sampling resolution for the X (azimuth) direction is M_a, there is

$$M_a = |V| / PRF \tag{6}$$

where $|V|$ is speed and PRF is the transmission frequency of azimuth beam.

In the image coordinates, if the image point coordinate (x, y) becomes to (x', y') because of measuring or matching error, the error dx=x–x' would lead to the change of the interpolation time of the sensor state vector and interpolation time of attitude data (Fig. 2).

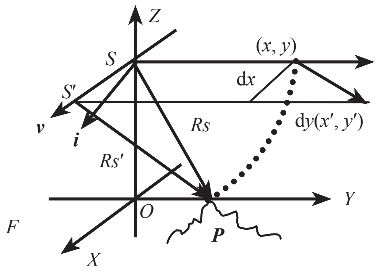

Fig. 2 The geometry relationship of image point measurement error

For the change of interpolation time caused by the errors is relatively small, it can be considered as no change to the attitude value. The time error mainly affects the location of the sensor. Let the sensor location changing from S to S' and for the coplanar Eq. (5) there is

$$\mathrm{d}F_C = \vec{i} \cdot \mathrm{d}(\overrightarrow{OS} - \overrightarrow{OP}) = \vec{i} \cdot \mathrm{d}\overrightarrow{OS} = \vec{i} \cdot \overrightarrow{SS'} = \cos(\vec{i}, \vec{v}) M_a \mathrm{d}x$$

where $\vec{i}$ is the unit vector of normal vector of the beam plane and $\vec{v}$ is the unit vector of the velocity vector. Set β as the angle between the normal vector and the velocity vector, so

$$\mathrm{d}F_C = M_a \cos\beta \cdot \mathrm{d}x \tag{7}$$

Let measurement accuracy of the image point coordinates is m_0, so the effect to virtual observation accuracy of coplanar equation conditions caused by the measurement accuracy can be expressed as

$$m_{F_C} = M_a \cos\beta \cdot m_0$$

Let the mean square error of unit weight is m_0, then the weight of the virtual observation value for coplanar equation (Eq. (5)) is as blow.

$$p_{F_C} = (m_0 / m_{F_C})^2 = \frac{1}{(M_a \cos\beta)^2} \tag{8}$$

From Eq. (7), it is known as

$$\mathrm{d}x = \frac{1}{M_a \cos\beta} \mathrm{d}F_C$$

The original coplanarity equation in Eq. (5) is still right when it is multiplied by a coefficient $-1/(M_a\cos\beta)$ for both sides, here the weight for new virtual observation value and for measured value of the image point is the same. At the same time, the theoretical error for image point coordinates is equal to that of virtual observation values from the revised equation. Therefore the improved R-Cp equation with explicit function form of image point coordinates is

$$\begin{cases} x = [(X - Xs)(\cos\varphi\cos k) + (Y - Ys)\sin k - \\ \quad (Z - Zs)(\sin\varphi\cos k)] / (M_a \cos\beta) = 0 \\ y = \left[\sqrt{(X - Xs)^2 + (Y - Ys)^2 + (Z - Zs)^2} - R_0\right] / M_r \end{cases} \tag{9}$$

For side-looking radar, velocity vector is consistent to the normal vector of the beam plane and the value of $\cos\beta$ is higher than 0.996 with the attitude angle less than 5°. To side-looking radar imagery $\cos\beta$ can be replaced by 1.0 and now compared with image measurement error the calculation error can be ignored, then the coplanarity equation can be simplified further. Usually the image coordinate is transformed to the sensor coordinate system while processing optical imagery and the unit for (x, y) is the unit of length. In this study the unit for (x, y) from SAR image is pixel which make it inconvenient to digital photogrammetric survey combining with SAR imagery and optical imagery. Let the size of the equivalent pixel from the physical sensor is μ_0 and then both sides of the range and coplanarity equations expressed by Eq. (9) are multiplied by the value, the equations could be converted to the explicit function equations of the image point coordinates in the equivalent physical sensor space.

3 RANGE AND COPLANARITY EQUATION EXPRESSED IN THE GEOCENTRIC RECTANGULAR COORDINATE SYSTEM

In general, satellite position $\vec{P}(t_i)$ and velocity values $\vec{V}(t_i)$ in the earth-fixed geocentric rectangular coordinate system (such as WGS84) are provided by the auxiliary data of SAR imagery. In other words, reference datum of the state vector is earth-fixed geocentric rectangular coordinate system. The reference datum of the attitude of the three-axis stabilized satellite is orbit coordinate system (Zhang, 1998). In the geocentric coordinate system, the mathematical definition expression of the three-axis of the orbital coordinate system is as follows (France SPOT Image Company, 2002).

$$\begin{cases} \vec{Z}_O = [(Z_O)_X, (Z_O)_Y, (Z_O)_Z] = \vec{P}(t) / \|\vec{P}(t)\| \\ \vec{Y}_O = [(Y_O)_X, (Y_O)_Y, (Y_O)_Z] = [\vec{Z}_O \times \vec{V}(t)] / \|\vec{Z}_O \times \vec{V}(t)\| \\ \vec{X}_O = [(X_O)_X, (X_O)_Y, (X_O)_Z] = \vec{Y}_O \times \vec{Z}_O \end{cases} \tag{10}$$

The formula above expresses the orbital coordinate system O-$X_O Y_O Z_O$ which is also shown in Fig. 3; X_O, Y_O, Z_O with X, Y, Z as subscript represent the components of the X_O, Y_O, Z_O in three directions of X, Y, Z in the geocentric rectangle coordinate system. Therefore, the conversion matrix $\boldsymbol{R}_O^E$ from the orbital coordinate system to the geocentric rectangle coordinate system is as follows.

$$\boldsymbol{R}_O^E = \begin{bmatrix} (X_O)_X & (Y_O)_X & (Z_O)_X \\ (X_O)_Y & (Y_O)_Y & (Z_O)_Y \\ (X_O)_Z & (Y_O)_Z & (Z_O)_Z \end{bmatrix} \tag{11}$$

So in geocentric rectangle coordinate system the unit normal

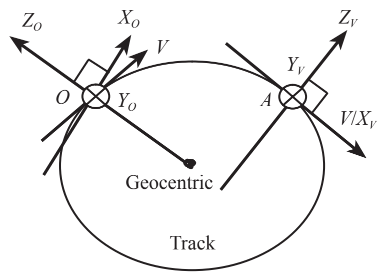

Fig. 3 Orbital coordinate system and flight coordinate system

vector $\vec{i}$: ($i_X\ i_Y\ i_Z$) for the beam plane can be calculated as follows.

$$\vec{i} = \begin{bmatrix} i_X & i_Y & i_Z \end{bmatrix}^{\mathrm{T}} = \boldsymbol{R}_{\boldsymbol{O}}^{E}\ \boldsymbol{R}_{\boldsymbol{b}}^{\boldsymbol{O}} \begin{bmatrix} 1 & 0 & 0 \end{bmatrix}^{\mathrm{T}} \tag{12}$$

where $\boldsymbol{R}_O^E$ is the conversion matrix from the orbital coordinate system to the geocentric rectangle coordinate system, and $\boldsymbol{R}_b^O$ is the conversion matrix from the satellite body coordinate system to orbital coordinate system, $[1\ 0\ 0]^{\mathrm{T}}$ is the unit vector of x axes in satellite body coordinate system. Accordingly in the geocentric rectangle coordinate system the R-Cp equation can be expressed as

$$\begin{cases} (X-Xs)^2+(Y-Ys)^2+(Z-Zs)^2-(yM_r+R_0)^2=0 \\ i_X(X-Xs)+i_Y(Y-Ys)+i_Z(Z-Zs)=0 \end{cases} \tag{13}$$

where $\cos\beta=\cos(\vec{i},\vec{v})=\cos\varphi\cos k$, (φ, k) are the attitude angle parameters, then the R-Cp model with explicit function form of image coordinate is

$$\begin{cases} x=\left[i_X\cdot(X-Xs)+i_Y\cdot(Y-Ys)+i_Z\cdot(Z-Zs)\right]/ \\ \quad (M_a\cos\varphi\cos k)=0 \\ y=\left[\sqrt{(X-Xs)^2+(Y-Ys)^2+(Z-Zs)^2}-R_0\right]/M_r \end{cases} \tag{14}$$

Take the increment of the initial data of exterior orientation parameters (Xs, Ys, Zs, φ, k) and the ground point coordinates as unknown values and the general form of error equation for the image point measurement coordinates can be written as below.

$$\begin{cases} v_x=f_{1Xs}\Delta Xs+f_{1Ys}\Delta Ys+f_{1Zs}\Delta Zs+f_{1\varphi}\Delta\varphi+f_{1k}\Delta k+ \\ \quad f_{1X}\Delta X+f_{1Y}\Delta Y+f_{1Z}\Delta Z-l_x \qquad p_x \\ v_y=f_{2Xs}\Delta Xs+f_{2Ys}\Delta Ys+f_{2Zs}\Delta Zs+f_{2\varphi}\Delta\varphi+f_{2k}\Delta k+ \\ \quad f_{2X}\Delta X+f_{2Y}\Delta Y+f_{2Z}\Delta Z-l_y \quad p_y \end{cases} \tag{15}$$

where v_x, v_y are error increment of the image point coordinates in azimuth and range direction, $f_{..}$ are the coefficients of the error equation, l_x, l_y are constants, p_x and p_y are weights of the corresponding measurement coordinates and can be calculated by point measurement accuracy.

For optical imagery (x_0, y_0) are coordinates of principal point in the image. Though there is no actual radar sensor image space (Δx_0, Δy_0) still can be found with a specific geometric physical meaning to side-looking radar imagery. Δx_0 can lead shift for beam center plane, and Δy_0 have the same effect as the initial slant range system error. When positioning with side-looking radar imagery there are system errors in azimuth and slant range directions caused by SAR sensor, Δx_0, Δy_0 can still play its roles when calibrating radar sensor.

4 RIGOROUS POSITIONING MODEL FOR SPACEBORNE SAR IMAGERY

The following SAR image positioning directly refer to the model and method for optical imagery positioning with sparse control point.

The refinement model of orbit and attitude can be established with a linear polynomial as

$$\begin{cases} X_S=X_{S0}+a_0+a_1t \\ Y_S=Y_{S0}+b_0+b_1t \\ Z_S=Z_{S0}+c_0+c_1t \\ \varphi=\varphi_0+f_0+f_1t \\ k=k_0+g_0+g_1t \end{cases} \tag{16}$$

where (X_{S0}, Y_{S0}, Z_{S0}, ω_0, k_0) is the initial sensor location and attitude value; a_i, b_i, c_i, f_i, g_i(i=0, 1, ···, n) are refinement parameters for orbit and attitude data.

The Eq. (17) is based on error equations of the image point measurement coordinates, ground point observation coordinates, observation orbit and attitude. And it can be solved by the least square method.

$$\begin{cases} \boldsymbol{V}_{xy}=\boldsymbol{B}_g\boldsymbol{g}+\boldsymbol{B}_t\boldsymbol{t}-\boldsymbol{L}_{xy}\ldots\boldsymbol{P}_{xy} \\ \boldsymbol{V}_g=\boldsymbol{E}_g\boldsymbol{g} \qquad -\boldsymbol{L}_g\ldots\boldsymbol{P}_g \\ \boldsymbol{V}_t= \qquad \boldsymbol{E}_t\boldsymbol{t}-\boldsymbol{L}_t\ldots\boldsymbol{P}_t \end{cases} \tag{17}$$

where $\boldsymbol{V}$ is correction vector of the observation, error equation $\boldsymbol{V}_{xy}$ is correction vector of image point measurement coordinate, $\boldsymbol{V}_g$ is correction vector of ground point observation coordinate, $\boldsymbol{V}_t$ is correction vector of orbit attitude observation; and $\boldsymbol{g}$, $\boldsymbol{t}$ are unknown vectors want to be solved, $\boldsymbol{g}$ [ΔX, ΔY, ΔZ] represents the ground point coordinate increment; $\boldsymbol{t}$ [a_0, b_0, c_0, e_0, f_0, a_1, b_1, c_1, e_1, f_1] is the polynomial coefficients for the orbit attitude refinement model; $\boldsymbol{B}_g$, $\boldsymbol{B}_t$, $\boldsymbol{E}_g$, $\boldsymbol{E}_t$ are matrixes for the error equation coefficients; $\boldsymbol{L}_{xy}$, $\boldsymbol{L}_g$, $\boldsymbol{L}_t$ are the constant vectors of the corresponding observation error equation; $\boldsymbol{P}_{xy}$, $\boldsymbol{P}_g$, $\boldsymbol{P}_t$ are the weight matrixes. $\boldsymbol{P}_{xy}$, $\boldsymbol{P}_g$ are the weights of image point measurement coordinates and ground point coordinates and calculated directly according to their observational accuracy. Here a_0, b_0, c_0, a_1, b_1, c_1 are refinement model parameters of orbit data and their accuracy is consistent with the measurement accuracy of sensor position and velocity. e_0, f_0, e_1, f_1 are refinement model parameters of roll angle and yaw angle and their accuracy is consistent with the attitude accuracy and attitude stability.

There is a good corresponding relationship between the parameters in the error equation group and actual geometric physical observations. Therefore the problem of weight setting can be solved smoothly.

5 TESTS AND ANALYSIS

5.1 Positioning test with TerraSAR-X imagery

The TerraSAR-X band data used in the test was imaged in July 2009, whose sampling resolution is 0.91 m in slant range direction and 2.06 m in azimuth direction. The region covered by the image lies in the Tibet with center coordinates (96.3°, 32.2°) and elevation changing from 3500 m to 4500 m. There are 15 ground points with known coordinates which are obtained by block adjustment method with SPOT5 HRS / HRG imagery based on RF model, and the tool is integration mapping software PixelGrid developed by China Academy Surveying and Mapping (Zhang, 2009).

TerraSAR-X images with 0 doppler which means there is a vertical relationship between beam center plane and the direction of the velocity. Here reference datum of the attitude is established within the flight coordinate system, in which the direction of the velocity $\boldsymbol{V}$ is taken as the X-axis direction (Fig. 3 $V\text{-}X_V Y_V Z_V$), and the mathematical definition is

$$\begin{cases} \vec{\boldsymbol{X}}_V = [(X_V)_X, (X_V)_Y, (X_V)_Z] = \vec{\boldsymbol{V}}(t) / \left\| \vec{\boldsymbol{V}}(t) \right\| \\ \vec{\boldsymbol{Y}}_V = [(Y_V)_X, (Y_V)_Y, (Y_V)_Z] = \vec{\boldsymbol{P}}(t) \times \vec{\boldsymbol{V}}(t) / \left\| \vec{\boldsymbol{P}}(t) \times \vec{\boldsymbol{V}}(t) \right\| \\ \vec{\boldsymbol{Z}}_V = [(Z_V)_X, (Z_V)_Y, (Z_V)_Z] = \vec{\boldsymbol{X}}_V \times \vec{\boldsymbol{Y}}_V \end{cases} \tag{18}$$

Therefore, the initial values of the attitude roll and yaw angle relative to the reference coordinate system are both 0. Referring $\boldsymbol{R}_O^E$ (Eq. (11)), rotation matrix $\boldsymbol{R}_V^E$ from attitude reference system to the geocentric coordinate system can be established. Normal vector of the beam center plane is

$$\vec{\boldsymbol{i}} = \begin{bmatrix} i_X & i_Y & i_Z \end{bmatrix}^{\mathrm{T}} = \boldsymbol{R}_V^E \ \boldsymbol{R}_b^V \begin{bmatrix} 1 & 0 & 0 \end{bmatrix}^{\mathrm{T}}$$

Take it into Eq. (14) and R-Cp equation for TerraSAR imagery can be easily re-established.

(1) Orientation and positioning test with different control points

In the test, the control points with different numbers and distributions are used, including

Case 1: no GCP;

Case 2: one GCP centered at the test area;

Case 3: four GCPs with one at each corner of the test area;

Case 4: nine GCPs evenly distributed.

In each case, the remaining points are used as check points. The weight of the parameters in the orbit attitude refinement model are set according to the accuracy with satellite orbit 60 m, speed 1 m/s, attitude 10" and attitude stability 0.5"/s. The image coordinate residuals of the control points and check points after orientation can be calculated directly with error Eq. (15). Their accuracy is showed in Table 1.

Table 1 Accuracy of orientation and positioning for single image

Model	Point attribute	The number of control points	0	1	4	9
Orientation and positioning accuracy with R-Cp model	Control points	Azimuth direction/ pixel		0.01	0.42	0.99
		Range direction/ pixel		0.03	0.49	1.57
		Plane /m		0.05	1.21	3.43
	Check points	Azimuth direction /pixel	3.80	1.45	1.28	1.11
		Range direction /pixel	38.36	2.30	2.19	2.09
		Plane /m	67.96	5.07	4.55	4.33
	Difference of residual error	Max $\lvert v_x^1 - v_x^2 \rvert$ /pixel	0.00	0.00	0.00	0.00
		Max $\lvert v_y^1 - v_y^2 \rvert$ /pixel	0.00	0.00	0.00	0.00
Orientation and positioning accuracy with R-D model	Control points	Azimuth direction /pixel		0.01	0.49	1.12
		Range direction /pixel		0.04	0.53	1.58
		Plane /m		0.07	1.37	3.61
	Check points	Azimuth direction /pixel	3.80	1.44	1.29	1.25
		Range direction /pixel	38.36	2.30	2.20	2.12
		Plane /m	67.96	5.06	4.58	4.53

Eq. (13) or Eq. (14) combining with the precise earth ellipsoid model (Eq. (19)), which considers the height factor, the corresponding ground point coordinates (X, Y, Z) in geocentric rectangle coordinate system can be calculated.

$$\frac{X^2 + Y^2}{(A+H)^2} + \frac{Z^2}{(B+H)^2} = 1 \tag{19}$$

where A is semi-major axis of the earth ellipsoid; B is the semi-minor axis of the earth ellipsoid; H is the elevation of the ground point which is extracted from the DEM data. To the WGS84 coordinate system, $A = 6378137.0$; $B = 6356752.314$.

After converting the calculated ground points coordinates to the Gaussian plane, the orthorectification of the original image can be done with resampling technique. In this test DEM data was extracted from SPOT5HRS/HRG image with PixelGrid software, the TerraSAR-X image was rectified based on original orientation parameters and refined orientation parameters. By counting the positioning residuals of the known 15 points, and the plane positioning accuracy for the control and check points are showed in Table 1 “Orientation and positioning accuracy with R-Cp model” row.

The results from the comparison method are also showed in the table. Here the method is based on R-D model, and take sensor position as unknown value, the linear refinement model (Eq. (17)) for orbit; and the velocity refined value is calculated according to derivation of the refined orbit to the time, a existing methods (Yuan, 2001; Yuan & Wu, 2009) is used to set the weight. The orientation residuals are calculated by traditional iteration ways and orthorectification method is as above for R-Cp model. The results are showed in Table 1 “Orientation and positioning accuracy with R-D model” row.

After the orthorectification with original orientation parameters and refined parameters from R-Cp model with one control point, the sketch map for residual vector and the distribution of the 15 ground points is shown in Fig. 4.

There are corresponding solved values for orientation parameters with different control points. When with one and nine control points, the absolute values of the orientation parameter increments in R-Cp model are showed in Table 2.

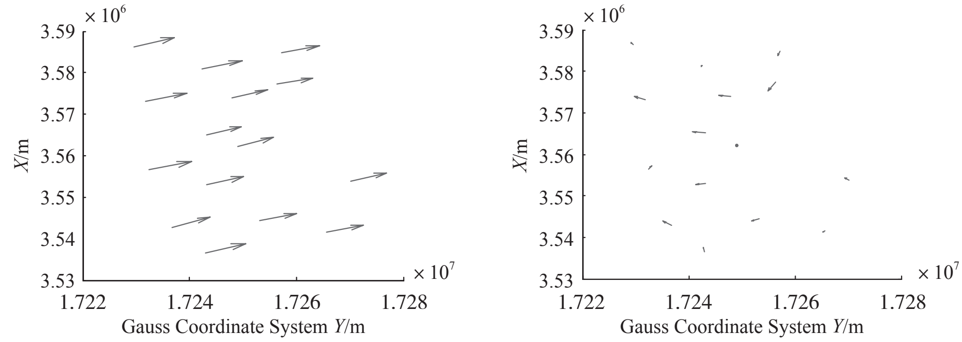

(a) Zero GCP (b) One GCP

Fig. 4 The sketch map of orientation residual vector and the distribution of control and check points

Table 2 The solved value of orientation parameters with one and nine control points

	a_0/m	b_0/m	c_0/m	e_0(")	f_0(")	a_1/(m/s)	b_1/(m/s)	c_1/(m/s)	e_1("/s)	f_1("/s)
one GCP	13.31	31.14	10.48	1.03	0.54	0.084	0.198	0.066	0.00236	0.00122
nine GCPs	4.28	40.01	8.51	3.32	9.20	0.187	0.104	0.506	0.03210	0.03182

In order to explore the correlation of the orientation parameters in R-Cp model, the coefficient matrix condition number of the normal equation is calculated. Take all 15 ground points as control points and five constant parameters and ten linear parameters in refinement model of the orbit-attitude (Eq. (17)) as unknown values, the error Eq. (15) and their normal equation were established. The condition number P_5 and P_{10} can be calculated as

$$P_5 = \lambda_{\max} / \lambda_{\min} = 5.10\times10^{13}/0.0042 = 1.21\times10^{16}$$
$$P_{10} = \lambda_{\max} / \lambda_{\min} = 1.07\times10^{15}/4.2127\times10^{-6} = 2.54\times10^{21} \quad (20)$$

where $\lambda_{\max}$ and $\lambda_{\min}$ are maximum and minimum eigenvalues of coefficient matrix of normal equation respectively.

(2) Comparison of image coordinate residual

Two methods are used to calculate the orientation residuals of the image points. One adopts Eq. (15) directly. The other calculates the theoretical coordinate(x^1, y^1) of the image point firstly and then the difference between them and the measured coordinates, whose detail steps are showed as below.

Step 1 According the initial image line x_n to interpolate the elements of exterior orientation (position and attitude of the sensor) at the corresponding time, and then to establish the equation of the beam plane center of side-looking radar: $\vec{i}\cdot(\overrightarrow{OP}-\overrightarrow{OS})=0$;

Step 2 To calculate the distance d for the ground point along the normal direction of the beam center plane to the plane. Stop the iterative search if the distance is less than a given threshold, and the current line x_n is theory coordinates x^1 of the image line of the corresponding ground point, then jump to Step 5;

Step 3 To re-estimate image line x_{n+1} of the point corresponding to ground point based point-surface distance d and azimuth resolution M_a of the image.

$$x_{n+1} = x_n + d / M_a \quad (21)$$

Step 4 To interpolate the corresponding orbit-attitude value based on the imaging time of the x_{n+1} line and re-start Step 2;

Step 5 To calculate the theoretical column coordinate y^1 of the image point with ground point coordinates and the position of SAR sensor.

$$y^1 = \left[\sqrt{(X-Xs)^2+(Y-Ys)^2+(Z-Zs)^2} - R_0\right] \Big/ M_r \quad (22)$$

where the orientation residuals v_x^1, v_y^1 is the difference between the theoretical value(x^1, y^1) and the measured value of the image point coordinates. Moreover the orientation residuals v_x^2, v_y^2 of all ground points were calculated by the Eq. (15). To make a subtract operation between the two residuals and get $|v_x^1-v_x^2|$ and $|v_y^1-v_y^2|$. Their maximums are showed in Table 1.

5.2 Test analysis

Although the data processing tests are relatively simple, they involves basic content about image photogrammetric adjustment algorithm. The follows can be obtained:

(1) When positioning with R-Cp model, with original orientation parameters and without ground control point the plane positioning accuracy in mountain areas is 68 m, and accuracy in along azimuth direction is higher than range direction. With one control point the image positioning accuracy is greatly improved to 5.1 m. With the increasing of control point number the accuracy still can be improved but with a relatively lower speed. The test proved that only with one control point the plane positioning accuracy can meet the requirement (plane 7.5 m) of the map of 1:10000 digital orthophoto criterion in mountain region formulated by surveying and mapping industry standards(National Bureau of Surveying and Mapping, 2010).

(2) In the test, for the TerraSAR-X imagery the accuracy of R-Cp

model and that of the R-D model are same without control point and similar with sparse control points. When there are more control points the accuracy of R-Cp model is slightly better than that of the R-D model. So in view of imaging geometry the two equations have coequal rigor to TerraSAR image.

(3) For the known points, their residuals calculated by the improved error equations and by iterative methods are identical which means the geometric imaging R-Cp model with the form of an explicit function of the point coordinates is correct. The improved error equations can be used to detect gross error for the image point measurement while solving orientation parameters. It also is proved that the weight setting for the improved R-Cp error equation according to pixel measurement accuracy is reasonable.

(4) When the condition number of a matrix is larger than 1000, the matrix is considered as ill-conditioned (Dunn, 1959). To spaceborne SAR imagery, the coefficient matrix condition number of the normal equation for the R-Cp error equation is far larger than 1000, so there is a strong correlationship between the orientation parameters. Generally there is a clear requirement for GCPs' least number while solving the rigorous model for spaceborne imagery. Even there is a large number of control points, the large deviation between original values and the solved values of the orientation parameters also can be caused by the ill-conditioned matrix. Table 2 shows that the improved R-Cp model for SAR image not only realize high precision positioning with sparse control points, but also overcome the strong correlation among the orientation parameters.

(5) Precise orientation is the key to the rigorous positioning for remote sense imagery. When stereo positioning and block adjustment with radar imagery and sparse control point the techniques and methods proposed in this study can be applied or learned, such as the improved R-Cp geometric imaging equation and the combined adjustment model.

6 CONCLUSIONS

Photogrammetric techniques and methods for optical imagery are far earlier than those for radar imagery. For optical imagery there have developed systematic and mature data processing models and methods based collinear equation. With the form of explicit function of the image point coordinate, the improved Range-Coplanarity equation proposed in this paper can absorb and utilize many of the mature digital photogrammetric processing methods for the optical imagery directly. By referring combined adjustment methods for optical imagery, rigorous positioning model for radar imagery with sparse control points is established which is rigorous, stable, efficient and beneficial to gross errors detection. Based on the proposed methods other techniques and methods for SAR imagery like geometry rectification, stereotactic positioning and block adjustment with sparse control points were developed and had been applied well in topographic mapping project at the scale of 1:50000 in western China, where many areas are perennially covered with clouds or snow and SAR image is the first selection for mapping. It can be showed from the theory and tests that the improved R-Cp geometric imaging equation and the established R-Cp rigorous positioning model can play their unique advantages in complex adjustment processing for multi-source data and can promote the theory and application level of radar imagery photogrammetry.

REFERENCES

Cheng C Q, Zhang J X, Deng K Z and Zhang L. 2012. Range-Coplanarity equation for radar geometric imaging. Journal of Remote Sensing, 16(1): 38–49

Cumming I G and Wong F H C. 2005. Digital Processing of Synthetic Aperture Radar Data: Algorithms and Implementation. Boston: Artech House, Inc

Dunn O J. 1959. Confidence intervals for the means of dependent, normally distributed variables. Journal of the American Statistical Association, 54(287): 613–621

France SPOT Image Company. 2002. SPOT Satellite Geometry Handbook, S-NT-73_12-SI, Edition 1, Revision 0. 15. 01. 2002

Johnsen H, Lauknes L and Guneriussen T. 1995. Geocoding of fast-delivery ERS-1 SAR image mode product using DEM data. International Journal of Remote Sensing, 16(11): 1957–1968 [DOI: 10.1080/01431169508954532]

Konecny G and Schuhr W. 1988. Reliability of Radar Image Data. 16th ISPRS, (16): 92–101

Leberl F. 1978. Radargrammetry for Image Interpretation. ITC Technical Report

Leberl F W. 1990. Radar Grammetric Image Processing. Norwood: Artech House

Shan J. 2002. Combined Adjustment for Photogrammetry and Non-photogrammetry Observation Data. Beijing: Surveying and Mapping Press: 96–115

State Burea of Surveying and Mapping. 2010. Surveying and Mapping Trade Criterion of PRC [CH/T 9009. 3-2010]. Digital products of fundamental geographic information 1:5000 1:10000 1:25000 1:50000 1:100000 digital orthophoto maps. 3–3

Tao B Z. 2001. Free Net Adjustment and Deformation Analysis. Wuhan: Wuhan Technical University of Surying and Mapping Publishing House: 1–77

Wang Z Z. 1979. Principle of Photogrammetry. Beijing: Surveying and Mapping Press: 93–103

You H J, Ding C B and Fu K. 2007. SAR image localization using rigorous SAR collinearity equation model. Acta Geodaetica et Cartographica Sinica, 36(2): 158–162

Yuan X X. 2001. Principle and Application of GPS-Supported Aerotriangulatiion. Beijing: Surveying and Mapping Press: 57–62

Yuan X X and Wu Y D. 2010. Object location of space-borne SAR imagery under lacking ground control points. Geomatics and Information Science of Wuhan University, 35(1): 88–91

Zhang L, Zhang J X, Chen X Y and An H. 2009. Block-adjustment with SPOT-5 imagery and sparse GCPs based on RFM. Acta Geodaetica et Cartographica Sinica, 38(4): 302–310

Zhang R W. 1998. Satellite Orbit-Attitude Dynamics and Controlling. Beijing: Beijing University of Aeronautics and Astronautics Publishing House: 137

侧视雷达影像距离-共面模型严密定位

程春泉，张继贤

中国测绘科学研究院对地观测技术国家测绘局重点实验室，北京 100039

摘 要：本文对现有侧视雷达遥感影像的几何构像模型在摄影测量应用中的不足进行了理论分析，以外方位元素作为定向参数，依次建立了像点坐标显函数形式的距离-共面(R-Cp)方程、地心直角坐标系中星载侧视雷达影像的距离-共面方程、以及星载侧视雷达遥感影像的严密定位模型，并进行了稀少控制点条件的星载TerraSAR-X影像定位试验。理论和试验表明，本文所建立的R-Cp严密定位模型，使得雷达影像像点量测坐标作为摄影测量观测值的属性得到体现，容易吸收和利用光学遥感影像基于共线方程模型发展起来的成熟的数字摄影测量数据处理方法，有利于提高雷达遥感影像摄影测量数据处理的严密性、稳定性、可靠性及数据处理效率。

关键词：距离-共面方程，侧视雷达，稀少控制点，严密定位，外方位元素，联合平差

中图分类号：P237 **文献标志码**：A

引用格式：程春泉，张继贤. 2012. 侧视雷达影像距离–共面模型严密定位. 遥感学报，16(5): 881–894

Cheng C Q and Zhang J X. 2012. Rigorous positioning with side-looking radar imagery based on Range-Coplanarity model. Journal of Remote Sensing, 16(5): 881–894

1 引 言

遥感影像的数字摄影测量主要以遥感影像的几何构像模型为基础展开。目前，雷达影像严密构像方程主要是基于传感器状态矢量和多普勒参数的模型，以及基于传感器状态矢量和姿态参数(外方位元素)的模型。Leberl F与R-D模型是目前侧视雷达影像严密定位中使用得最广泛的几何模型(Leberl，1978，1990；Johnsen 等，1995)；以外方位元素作为定向参数的模型除雷达共线方程(Konecny和Schuhr，1988;尤红建 等，2007)外，距离-共面(R-Cp)方程是一种简洁严密的几何构像模型，其根据距离条件和波束中心共面条件来构建(程春泉 等，2012)。

SAR信号成像主要有R-D、C-S、ω-K等成像模型和算法(Cumming和Wong，2005)，运动补偿采用不同的运行状态参考基准、信号成像采用不同的参数以及参数估计精度均会导致不同形式的SAR影像形变，决定了目前还没有能够通用于所有SAR影像的严密几何构像模型，不同几何构像模型均有一定的使用条件。R-D几何模型主要适用于R-D成像的雷达影像，R-Cp方程适用于真实孔径雷达影像，或与等效真实孔径雷达影像(在SAR成像时运动补偿参考的运行状态下以相同或等效成像参数获取的真实孔径雷达影像)有相同构像几何关系的SAR影像。

遥感影像的严密定位处理涉及传统摄影测量的两个基本内容，一是影像的几何构像模型，二是基于构像模型的数据平差处理。在使用范围内，R-D模型与R-Cp模型理论上均是严密的，形式也都很简洁，本身具备了作为侧视雷达遥感影像进行摄影测量数据处理的基础条件。但由于像点坐标信息隐藏在构像方程中，与光学遥感影像共线方程相比，两种构像模型在数据平差处理时，仍表现出了一定的不足，主要表现在：

(1) 严密的摄影测量平差方法(如光束法平差)是将像点量测坐标作为摄影测量观测值基本单元，根据量测误差为偶然误差、像点的定向残差(根据定向

收稿日期：2012-01-05；修订日期：2012-04-06

基金项目：国家自然科学基金(编号: 41071237)；国家高技术发展计划(863计划)(编号: 2011AA120401，2011AA120402)

第一作者简介：程春泉(1972—)，男，副研究员，主要从事航空航天光学与雷达遥感影像摄影测量理论与应用研究工作。E-mail: cspring@casm.ac.cn。

参数计算得到的像点理论坐标与量测坐标的差异)能直接体现其定位误差的特点，以像点定向残差v_x, v_y平方和最小为目标来实现定向参数的求解(王之卓，1971)。而R-D与R-Cp方程中，像点y坐标隐含在方程中，x坐标没有直接参数体现。根据距离方程、多普勒方程或共面方程等条件式列出的误差方程，一般称为虚拟观测值的误差方程，根据虚拟观测值误差v_R、v_{fD}、v_{Cp}的平方和最小来求解得到的定向参数，理论上不等于像点量测坐标的定向残差也能达到最小。

(2)人工或影像匹配获得的像点量测坐标为摄影测量观测值，通过摄影测量观测值与非摄影测量观测值间的联合平差是实现稀少控制点遥感影像严密定位的基本方法(袁修孝，2001；单杰，2002)，准确的定权对于提高测量平差未知数解算的稳定性、可靠性和精度，起着重要的作用(陶本藻，2001)。权与观测值的精度联系一起的，但虚拟观测值的误差方程不是针对摄影测量观测值，没有直接的“精度”信息，给多源观测数据的联合处理带来不便，甚至有损数据处理的严密性和精度。

(3)基于R-D和R-Cp方程的定位应用中通常构像方程条件式建立误差方程，像点坐标直接以量测值代入，没有类似基于共线方程模型误差方程中相应的像点坐标改正参数v_x，v_y，意味着平差解算时，各像点的定向残差不能在定向参数解算过程中由误差方程直接得出，在区域网影像中，匹配像点容易达到成千上万数目，传统通过迭代求解像点理论坐标的方法来求解量测误差，明显降低运算效率；而雷达遥感影像的量测误差通常情况下要远大于光学遥感影像，粗差的存在也给传统的验后方差定权方法带来干扰。定向过程中粗差的探测和剔除是影像摄影测量的重要内容，当前使用的几何构像模型给粗差探测带来不便。

由于R-Cp方程以外方位元素作为定向参数，只要将其改进成像点坐标显函数形式，基于共线方程模型发展起来的成熟的数字摄影测量数据处理方法，在雷达遥感影像中仍然能得到很好的吸收和利用。因此，本文首先以R-Cp方程为基础，推导如式(1)的侧视雷达影像几何构像方程，并在此方程基础上建立稳定、可靠、高效的侧视雷达遥感影像严密定位模型。

$$(x,y)=f_{xy}(Xs,Ys,Zs,\varphi,k,X,Y,Z) \tag{1}$$

式中，(x, y)为像点坐标，(X, Y, Z)为地面点坐标，(Xs, Ys, Zs)为传感器天线的空间坐标，φ为姿态俯仰角，k为偏航角。

2 像点坐标显函数形式的距离–共面方程

距离-共面条件是指一行影像对应的所有地面点均在该行影像摄影时刻天线发射的雷达波束中心面内，这个波束中心面由传感器状态矢量和姿态确定；传感器到地面目标点的空间距离与雷达波测量的距离相等。距离-共面方程根据式(2)建立(程春泉 等，2012)：

$$\begin{cases} R=|\overline{\boldsymbol{OP}}-\overline{\boldsymbol{OS}}| \\ \vec{\boldsymbol{i}}\cdot(\overline{\boldsymbol{OP}}-\overline{\boldsymbol{OS}})=0 \end{cases} \tag{2}$$

式中，$\vec{\boldsymbol{i}}$、$\overline{\boldsymbol{OP}}$、$\overline{\boldsymbol{OS}}$分别为波束中心面的法向量(即为传感器坐标系的$x$轴经姿态旋转后的$x'$轴)、地面点位置向量和传感器位置向量。$R$为雷达波测量斜距。$\varphi$-$k$-$\omega$姿态转角系统的距离-共面方程的展开式为：

$$\begin{cases} (X-Xs)(\cos\varphi\cos k)+(Y-Ys)\sin k- \\ (Z-Zs)(\sin\varphi\cos k)=0 \\ (X-Xs)^2+(Y-Ys)^2+(Z-Zs)^2-(yM_r+R_0)^2=0 \end{cases} \tag{3}$$

式中，M_r为距离向分辨率，R_0为最近端斜距，y为像元在影像上的列坐标。

距离方程中包含像点y坐标参数，很容易将其转换成y的显函数形式，即：

$$y=\left[\sqrt{(X-Xs)^2+(Y-Ys)^2+(Z-Zs)^2}-R_0\right]\Big/M_r \tag{4}$$

侧视雷达影像与光学线阵影像均靠传感器的移动实现推扫式成像，均属于多摄站投影。光学线阵影像的共线方程可以认为是两个平面方程构成，侧视雷达影像波束中心平面方程与光学影像垂直速度方向的平面方程是类似的(图1中SAB平面)，其与另一个平面方程及另一个距离方程，分别构成了光学影像的共线方程与侧视雷达遥感影像的距离－共面方程，如图1所

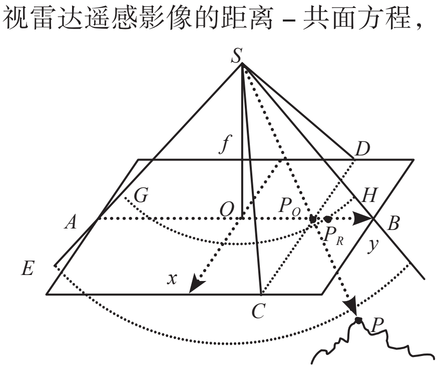

图1 距离-共面方程与共线方程的联系与区别

示。根据共线方程，地面目标点P的成像点在两个平面相交的直线SP_O上，根据R-Cp方程，则可理解成像点为在面和球相交的圆$GP_R H$上。

R-Cp模型中并不包含参数x。但根据共面方程，可以建立如下条件式：

$$F_C = \vec{\boldsymbol{i}} \cdot (\overrightarrow{\boldsymbol{OP}} - \overrightarrow{\boldsymbol{OS}}) = 0 \tag{5}$$

设X(方位)向的影像采样分辨率为M_a，令：

$$M_a = |V| / PRF \tag{6}$$

式中，$|V|$为速度大小，PRF为方位向脉冲重复频率。

在影像坐标系中，坐标为(x, y)的像点因量测或匹配误差，变为(x', y')，则量测误差$\mathrm{d}x=x-x'$导致传感器状态矢量和姿态数据内插时间的改变(图2)。由于量测误差导致的内插时间变化相对较小，姿态值在较短的时间内可认为没有变化，时间误差主要影响传感器的位置。设传感器位置由S变为S'，对共面条件式(5)而言，有：

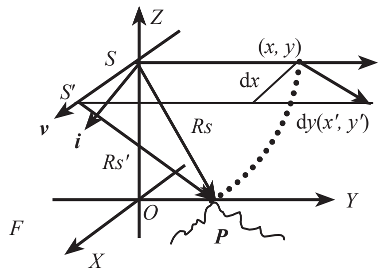

图2 像点量测误差几何

$$\mathrm{d}F_C = \vec{\boldsymbol{i}} \cdot \mathrm{d}(\overrightarrow{\boldsymbol{OS}} - \overrightarrow{\boldsymbol{OP}}) = \vec{\boldsymbol{i}} \cdot \mathrm{d}\overrightarrow{\boldsymbol{OS}} = \vec{\boldsymbol{i}} \cdot \overrightarrow{\boldsymbol{SS'}} = \cos(\vec{\boldsymbol{i}}, \vec{\boldsymbol{v}}) M_a \mathrm{d}x$$

式中，$\vec{\boldsymbol{i}}, \vec{\boldsymbol{v}}$分别为波束面法向量和速度向量的单位向量，同时令法向量与速度向量间的夹角为β，即$\cos\beta = \cos(\vec{\boldsymbol{i}}, \vec{\boldsymbol{v}}) = |i_X v_X + i_Y v_Y + i_Z v_Z|$，故有：

$$\mathrm{d}F_C = M_a \cos\beta \cdot \mathrm{d}x \tag{7}$$

设像点坐标的量测精度m_0，故像点量测精度对共面方程条件式虚拟观测值精度的影响为：

$$m_{F_C} = M_a \cos\beta \cdot m_0$$

当单位权中误差取m_0时，共面方程条件式虚拟观测值误差方程的权为：

$$p_{F_C} = (m_0 / m_{F_C})^2 = \frac{1}{(M_a \cos\beta)^2} \tag{8}$$

由式(7)知：

$$\mathrm{d}x = \frac{1}{M_a \cos\beta} \mathrm{d}F_C$$

在原共面方程两边同时乘以系数$-1/(M_a\cos\beta)$，方程仍成立，但虚拟观测值与像点量测值的权相同。同时，在定向参数迭代计算趋于理论真值的情况下，变换后的虚拟观测值误差与像点量坐标误差完全一致。因此，改进后的像点坐标显函数形式的R-Cp方程为：

$$\begin{cases} x = [(X - Xs)(\cos\varphi\cos k) + (Y - Ys)\sin k - \\ \quad (Z - Zs)(\sin\varphi\cos k)] / (M_a \cos\beta) = 0 \\ y = \left[\sqrt{(X - Xs)^2 + (Y - Ys)^2 + (Z - Zs)^2} - R_0\right] / M_r \end{cases} \tag{9}$$

对于正侧视雷达，速度方向与波束面法向量是一致的，姿态角度不超过5°时，cosβ值大于0.996。故一般情况下对于正侧视雷达影像，其取值可为常数1.0，对像点坐标误差计算的影响相对于其量测精度是可以忽略的，此时共面方程可得到进一步简化。对于光学影像，数据处理时通常将影像坐标转换到传感器坐标系中进行，(x, y)的单位通常是长度单位，而本文SAR影像坐标(x, y)的单位为像元，在涉及SAR影像与光学遥感影像联合定位时，带来不便。可假设物理传感器的等效像元大小为μ_0，式(9)表达的距离与共面方程两边均乘以该值，则可转化为等效物理传感器中像点坐标显函数形式的方程。

3 地心直角坐标系中的距离–共面方程

一般情况下，卫星辅助数据中提供了地固地心直角坐标系(如WGS84)中卫星位置$\vec{\boldsymbol{P}}(t_i)$和速度值$\vec{\boldsymbol{V}}(t_i)$，即状态矢量的参考基准为地固地心直角坐标系。对地定向的三轴稳定遥感卫星姿态参考基准为轨道坐标系(章仁为，1998)，在地心坐标系下，轨道坐标系三轴的数学定义表达式(France SPOT Image Company，2002)为：

$$\begin{cases} \vec{\boldsymbol{Z}}_{\boldsymbol{O}} = [(Z_O)_X, (Z_O)_Y, (Z_O)_Z] = \vec{\boldsymbol{P}}(t) / \|\vec{\boldsymbol{P}}(t)\| \\ \vec{\boldsymbol{Y}}_{\boldsymbol{O}} = [(Y_O)_X, (Y_O)_Y, (Y_O)_Z] = [\vec{\boldsymbol{Z}}_{\boldsymbol{O}} \times \vec{\boldsymbol{V}}(t)] / \|\vec{\boldsymbol{Z}}_O \times \vec{\boldsymbol{V}}(t)\| \\ \vec{\boldsymbol{X}}_{\boldsymbol{O}} = [(X_O)_X, (X_O)_Y, (X_O)_Z] = \vec{\boldsymbol{Y}}_{\boldsymbol{O}} \times \vec{\boldsymbol{Z}}_{\boldsymbol{O}} \end{cases} \tag{10}$$

上式表达的是图3中的轨道坐标系O-$X_O Y_O Z_O$，$(X_O)X$，$(Y_O)Y$，$(Z_O)Z$的下标X，Y，Z表示轨道坐标系三轴矢量(X_O)，(Y_O)，(Z_O)在地心直角坐标系三轴X，Y，Z方向的分量。因此，轨道坐标系到地心直角坐

标系的转换矩阵$\boldsymbol{R}_O^E$为：

$$\boldsymbol{R_O^E} = \begin{bmatrix} (X_O)_X & (Y_O)_X & (Z_O)_X \\ (X_O)_Y & (Y_O)_Y & (Z_O)_Y \\ (X_O)_Z & (Y_O)_Z & (Z_O)_Z \end{bmatrix} \tag{11}$$

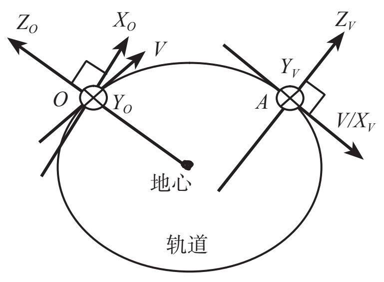

图3 轨道坐标系与飞行坐标系

因此，在地心直角坐标系中，波束中心面单位法向量$\vec{\boldsymbol{i}}$: $(i_X\ \ i_Y\ \ i_Z)$计算式为：

$$\vec{\boldsymbol{i}} = \begin{bmatrix} i_X & i_Y & i_Z \end{bmatrix}^{\mathrm{T}} = \boldsymbol{R_O^E}\ \boldsymbol{R_b^O} \begin{bmatrix} 1 & 0 & 0 \end{bmatrix}^{\mathrm{T}} \tag{12}$$

式中，$\boldsymbol{R_O^E}$，$\boldsymbol{R_b^O}$分别为轨道坐标系到地心直角坐标系、卫星本体坐标系到轨道坐标系的转换矩阵。相应地，地心直角坐标系中R-Cp方程的形式为：

$$\begin{cases} (X-Xs)^2+(Y-Ys)^2+(Z-Zs)^2-(yM_r+R_0)^2=0 \\ i_X(X-Xs)+i_Y(Y-Ys)+i_Z(Z-Zs)=0 \end{cases} \tag{13}$$

考虑到$\cos\beta=\cos(\vec{\boldsymbol{i}},\vec{\boldsymbol{v}})=\cos\varphi\cos k$, (φ, k)为姿态角，相应显函数形式的R-Cp模型为：

$$\begin{cases} x=\left[i_X\cdot(X-Xs)+i_Y\cdot(Y-Ys)+i_Z\cdot(Z-Zs)\right]/ \\ \quad (M_a\cos\varphi\cos k)=0 \\ y=\left[\sqrt{(X-Xs)^2+(Y-Ys)^2+(Z-Zs)^2}-R_0\right]/M_r \end{cases} \tag{14}$$

以外方位元素(Xs, Ys, Zs, φ, k)和地面点坐标(X, Y, Z)初值增量作为未知数，像点量测坐标误差方程式的一般形式可写为：

$$\begin{cases} v_x=f_{1Xs}\Delta Xs+f_{1Ys}\Delta Ys+f_{1Zs}\Delta Zs+f_{1\varphi}\Delta\varphi+f_{1k}\Delta k+ \\ \quad f_{1X}\Delta X+f_{1Y}\Delta Y+f_{1Z}\Delta Z-l_x \qquad p_x \\ v_y=f_{2Xs}\Delta Xs+f_{2Ys}\Delta Ys+f_{2Zs}\Delta Zs+f_{2\varphi}\Delta\varphi+f_{2k}\Delta k+ \\ \quad f_{2X}\Delta X+f_{2Y}\Delta Y+f_{2Z}\Delta Z-l_y \qquad p_y \end{cases} \tag{15}$$

式中，v_x，v_y分别为方位向和距离向像点坐标的误差增量，$f_{..}$为误差方程式系数，l_x，l_y方位向和距离向误差方程的常数项，p_x与p_y为相应量测坐标的权，根据像点量测精度计算即可。

在光学遥感影像中，(x_0, y_0)代表像主点坐标，在雷达传感器中，并没有实际的传感器像空间，但$(\Delta x_0, \Delta y_0)$在侧视雷达遥感影像中仍然可以找到具体的几何物理意义。Δx_0对影像成像几何的影响是引起波束中心面的平移，Δy_0则与初始斜距系统差影响相同，侧视雷达影像的定位在方位向和斜距向存在系统差时，两参数仍可以在传感器检校中发挥作用。

4 星载SAR影像严密定位模型

以下直接采用光学遥感影像稀少控制点的定位模型和方法，轨道姿态精化模型采用线性多项式，即：

$$\begin{cases} X_S=X_{S0}+a_0+a_1t \\ Y_S=Y_{S0}+b_0+b_1t \\ Z_S=Z_{S0}+c_0+c_1t \\ \varphi\ =\varphi_0+f_0+f_1t \\ k=k_0+g_0+g_1t \end{cases} \tag{16}$$

式中，$(X_{S0}, Y_{S0}, Z_{S0}, \omega_0, k_0)$为星历姿态数据初值，$a_i$, b_i, c_i, f_i, $g_i(i=0, 1, \cdots, n)$为星历姿态多项式精化模型参数。

将像点量测坐标误差方程式、地面点坐标观测值和轨道姿态观测值误差方程式一起，形成方程组(18)，并通过最小二乘求解。

$$\begin{cases} \boldsymbol{V_{xy}}=\boldsymbol{B_g g}+\boldsymbol{B_t t}-\boldsymbol{L_{xy}}\dots\boldsymbol{P_{xy}} \\ \boldsymbol{V_g}=\boldsymbol{E_g g} \qquad -\boldsymbol{L_g}\dots\boldsymbol{P_g} \\ \boldsymbol{V_t}= \qquad \boldsymbol{E_t t}-\boldsymbol{L_t}\dots\boldsymbol{P_t} \end{cases} \tag{17}$$

式中，$\boldsymbol{V}$代表观测值改正向量，$\boldsymbol{V_{xy}}$, $\boldsymbol{V_g}$, $\boldsymbol{V_t}$误差方程式分别为像点坐标、地面点坐标、轨道姿态观测值误差方程式，$\boldsymbol{P_{xy}}$, $\boldsymbol{P_g}$, $\boldsymbol{P_t}$为权矩阵，$\boldsymbol{g}$代表地面点坐标增量未知数向量$[\Delta X, \Delta Y, \Delta Z]$，$\boldsymbol{t}$代表轨道(航迹)姿态精化模型的一般多项式系数未知数向量$[a_0, b_0, c_0, e_0, f_0, a_1, b_1, c_1, e_1, f_1]$，$\boldsymbol{L_{xy}}$, $\boldsymbol{L_g}$, $\boldsymbol{L_t}$为相应观测值误差方程常数向量，$\boldsymbol{B_g}$、$\boldsymbol{B_t}$、$\boldsymbol{E_g}$、$\boldsymbol{E_t}$为误差方程系数设计矩阵。$\boldsymbol{P_{xy}}$、$\boldsymbol{P_g}$代表像点量测坐标和地面点坐标的权，直接按观测精度计算给出。$a_0, b_0, c_0, a_1, b_1, c_1$为星历数据精化模型参数，其精度分别与传感器位置和速度测量精度一致，e_0, f_0, e_1, f_1为侧滚角与偏航角的精化模型参数，其精度与姿态测量精度及姿态稳定度一致。因此，误差方程中组参数均能与相应的几何物理观测量对应起来，其定权问题能够得到顺利解决。

5 试验与分析

5.1 TerraSAR-X定位试验

试验采用星载TerraSAR-X波段影像,数据获取于2009年7月，斜距向采样分辨率为0.91 m，方位向采样分辨率为2.06 m。影像中心地理经纬坐标为(96.3°, 32.2°)，位属中国西藏自治区，影像覆盖区域的地面高程在3500 m至4500 m之间。影像上有已知坐标的地面点15个，通过中国测绘科学研究院一体化测图软件PixelGrid以RF模型对SPOT 5光学HRS/HRG影像加密方式获得(张力，2009)。

由于TerraSAR-X以0多普勒成像，意味着波束中心面与速度方向垂直。因此，此处将姿态参考基准建立在以速度V的方向为X轴的飞行坐标系上(图3中V–$X_VY_VZ_V$)，数学定义如下：

$$\begin{cases}\vec{\boldsymbol{X}}_V=[(X_V)_X,(X_V)_Y,(X_V)_Z]=\vec{\boldsymbol{V}}(t)/\left\|\vec{\boldsymbol{V}}(t)\right\| \\ \vec{\boldsymbol{Y}}_V=[(Y_V)_X,(Y_V)_Y,(Y_V)_Z]=\vec{\boldsymbol{P}}(t)\times\vec{\boldsymbol{V}}(t)/\left\|\vec{\boldsymbol{P}}(t)\times\vec{\boldsymbol{V}}(t)\right\| \\ \vec{\boldsymbol{Z}}_V=[(Z_V)_X,(Z_V)_Y,(Z_V)_Z]=\vec{\boldsymbol{X}}_V\times\vec{\boldsymbol{Y}}_V\end{cases} \quad (18)$$

因此，相对于此参考坐标系的姿态值仰角与偏航角初值均为0，姿态参考系到地心坐标系的旋转矩阵$\boldsymbol{R}_V^E$可参考$\boldsymbol{R}_O^E$(式(11))建立。则波束中心面法向量：

$$\vec{\boldsymbol{i}}=\begin{bmatrix}i_X & i_Y & i_Z\end{bmatrix}^{\mathrm{T}}=\boldsymbol{R}_V^E\ \boldsymbol{R}_b^V\ \begin{bmatrix}1 & 0 & 0\end{bmatrix}^{\mathrm{T}}$$

将上式代入式(14)中，即得地心直角坐标系R-Cp方程。

(1)不同数目控制点定向定位试验

试验分别采用不同数目和分布的控制点进行试验，分别包括0个、1个(中心点)、4个(角点)、9个点作为控制点，其余作为检查点。卫星轨道、速度、姿态及姿态稳定度分别按60 m，1 m/s，10″，0.5″/s精度值对轨道姿态精化模型中各参数观测值定权。在定向参数解算过程中，根据误差方程式(15)直接计算得到定向后控制点和检查点的像点残差，并统计它们的定向精度填于表1中。

以原始定向参数和精化后的定向参数为基础，结合PixelGrid对SPOT 5光学影像提取的DEM数据，将TerraSAR-X影像纠正到高斯平面。像点坐标对应的地物点地心直角坐标系坐标(X, Y, Z)的计算，通过式(13)联合考虑高程因子的精度无损地球椭球模型式(19)来进行。

$$\frac{X^2+Y^2}{(A+H)^2}+\frac{Z^2}{(B+H)^2}=1 \quad (19)$$

式中，A为地球椭球的长半轴，B为地球椭球的短半轴，H为地面点的高程，从DEM数据中提取。对于WGS84坐标系，A=6378137.0，B=6356752.314。

将计算得到的地面点坐标转换到高斯平面中，并通过重采样技术，实现原始影像的正射纠正。统计15个已知点的定位残差，计算相应控制点和检查点的平面定位精度，统计于表1“平面定位精度”栏中。

作为比较，以R-D模型为基础，以传感器位置作为未知数，轨道仍采用式(17)中的线性精化模型，速度精化值则根据精化后的轨道对时间求导获得，定权采用文献(袁修孝，2001;袁修孝和吴颖丹，2010)中的方法，所得到的相应结果一并统计于表1中。

表1 单片定向与定位精度统计

试验内容	点属性	控制点个数	0	1	4	9
R–Cp 模型精度	控制点	方位向定向精度/像元		0.01	0.42	0.99
		距离向定向精度/像元		0.03	0.49	1.57
		平面定位精度/m		0.05	1.21	3.43
	检查点	方位向定向精度/像元	3.80	1.45	1.28	1.11
		距离向定向精度/像元	38.3	2.30	2.19	2.09
		平面定位精度/m	67.9	5.07	4.55	4.33
		Max $\lvert v_x^1-v_x^2\rvert$/像元	0.00	0.00	0.00	0.00
		Max $\lvert v_y^1-v_y^2\rvert$/像元	0.00	0.00	0.00	0.00
R–D 模型精度	控制点	方位向定向精度/像元		0.01	0.49	1.12
		距离向定向精度/像元		0.04	0.53	1.58
		平面定位精度/m		0.07	1.37	3.61
	检查点	方位向定向精度/像元	3.80	1.44	1.29	1.25
		距离向定向精度/像元	38.3	2.30	2.20	2.12
		平面定位精度/m	67.9	5.06	4.58	4.53

图4为采用原始定向参数和采用1个控制点利用R-Cp模型对原始影像进行正射纠正后15个地面点的分布及残差矢量示意图。

使用不同控制点均得到相应的定向参数解算值，当采用1个和9个控制点时，R-Cp模型各定向参数精化值的绝对值统计于表2中。

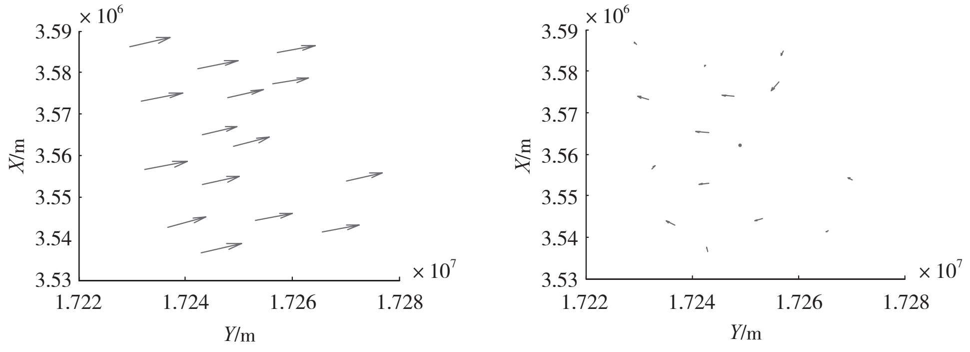

(a) 0个GCP　　(b) 1个GCP

图4　0个和1个GCP时控制检查点的分布及定位残差矢量示意图

表2　1个和9个控制点时定向参数解算值

	a_0/m	b_0/m	c_0/m	e_0(″)	f_0(″)	a_1/(m/s)	b_1/(m/s)	c_1/(m/s)	e_1(″/s)	f_1(″/s)
1个GCP	13.31	31.14	10.48	1.03	0.54	0.084	0.198	0.066	0.00236	0.00122
9个GCPs	4.28	40.01	8.51	3.32	9.20	0.187	0.104	0.506	0.03210	0.03182

为了考察R-Cp模型定向参数间的相关性，对以误差方程式(15)为基础建立的法方程条件数进行了计算，15个地面点均作为控制点，分别取轨道姿态精化模型式(17)中的5个常数项参数和10个线性参数作为未知数构建误差方程和法方程，按下式计算相应法方程的条件数P_5和P_{10}：

$$\begin{aligned} P_5 &= \lambda_{\max}/\lambda_{\min} = 5.10\times10^{13}/0.0042=1.21\times10^{16} \\ P_{10} &= \lambda_{\max}/\lambda_{\min} = 1.07\times10^{15}/4.2127\times10^{-6}=2.54\times10^{21} \end{aligned} \tag{20}$$

式中，$\lambda_{\max}$、$\lambda_{\min}$为法方程最大最小特征值。

(2)定向残差比较试验

采用两种方法计算像点的定向残差，一是直接利用式(15)，另一是采用如下迭代方法求地面点在原始影像上的像点理论坐标，并比较像点理论坐标与量测坐标间的差异，计算像点的定向残差：

步骤1　根据初始影像行x_n内插相应时刻的外方位元素，即传感器位置和姿态，并根据传感器位置和姿态建立侧视雷达波束中心面方程：$\vec{i}\cdot(\overrightarrow{OP}-\overrightarrow{OS})=0$；

步骤2　计算地面点沿着波束中心面法线方向到波束中心面的距离d。当距离小于给定的阈值时，停止迭代搜索，当前行x_n即为相应地面点影像行理论坐标x^1，跳到步骤5；

步骤3　根据点面距离d以及影像方位向分辨率M_a重新估计地面点对应的像点所在影像行x_{n+1}：

$$x_{n+1}=x_n+d/M_a \tag{21}$$

步骤4　根据第x_{n+1}行影像时刻内插相应的轨道姿态值，重复开始步骤2的操作；

步骤5　根据地面点坐标和相应影像行摄影时刻传感器位置，计算像点理论列坐标y^1。

$$y^1=\left[\sqrt{(X-Xs)^2+(Y-Ys)^2+(Z-Zs)^2}-R_0\right]\Big/M_r \tag{22}$$

以得到的精化后定向参数为基础，按上述迭代的方法求解地面点对应像点坐标的理论值(x^1, y^1)，理论值和测量值间的差异，为定向残差v_x^1，v_y^1。同时，根据式(15)计算所有地面点的定向残差v_x^2，v_y^2，将这两种方法获得的像点量测误差相减取绝对值$|v_x^1-v_x^2|$，$|v_y^1-v_y^2|$，将其最大值统计于表1中的Max$|v_x^1-v_x^2|$和Max$|v_y^1-v_y^2|$栏中。

5.2　试验分析

本文的数据处理试验虽较简单，但涉及影像严密定位和摄影测量平差(空中三角测量)算法的基本内容，可以看出：

(1)R-Cp模型在使用无控制点条件下的原始定向参数进行定位时，高山地区影像平面定位精度达到68 m，且方位(沿轨)向精度明显高于距离向精度；在有1个控制点的情况下，影像定位精度即得到大幅度

提高，精度达到5.1 m；随着控制点数目的增加，精度仍有所提高，但提高的速度较慢。试验表明，有1个控制点时，平面定位精度达到1∶1万高山地区数字正射影像图测绘行业标准要求的图上0.75 mm(平面7.5 m)精度要求(国家测绘局，2010)。

(2)本文试验中，在无控制点的情况下，TerraSAR-X影像R-Cp模型与R-D模型精度是相同的，在少量控制点的条件下，R-Cp模型与R-D模型精度基本一致，在控制点数目较多时，R-Cp模型定位精度略优于R-D模型。

(3)采用改进后的误差方程计算得到的各已知点残差与通过迭代方法计算得到的残差是完全相同的，表明本文像点坐标显函数形式的R-Cp几何构像模型是正确的，计算残差能够反应测量误差的大小，表明其在定向参数解算过程中可以用于像点量测粗差的探测，有利于粗差的发现，同时也表明根据像点量测精度对R-Cp方程的误差方程的定权是合理的。

(4)星载SAR影像R-Cp误差方程的法方程矩阵条件数远大于1000，而大于该值被认为存在严重相关性(Dunn，1959)。通常，星载影像对地定位严密模型的解算通常对地面控制点最少数目有明确要求，即使在大量控制点条件下，因方位元素间的强相关性会导致定向参数解算值与原始初值有很大的偏离，甚至无解。表2表明本文建立的定位模型解决了稀少控制点影像定位中的两个基本问题，即实现了稀少控制点条件下众多定向参数的解算，且克服了定向参数间的强相关性。

(5)遥感影像严密定位的关键均是实现影像的精确定向，表明本文改进的构像方程和构建的联合平差模型，以及相应的技术和方法可以应用或借鉴到稀少控制点雷达遥感影像立体定位、区域网平差等雷达遥感影像定位数据处理中。

6 结 论

光学遥感影像的摄影测量远早于雷达遥感影像，以共线方程为基础，光学影像已经有一套严密成熟的数字摄影测量数据处理模型和方法。本文建立的像点坐标为显函数形式的距离-共面方程，除误差方程的线性化方式有所区别外，可以直接吸收和利用光学线阵遥感影像基于共线方程模型发展起来的数字摄影测量处理方法。通过借鉴光学影像的联合平差方法，建立了一种真正意义上稀少控制点的雷达影像严密定位模型，在复杂的多源数据处理中能够发挥其严密、稳定、高效及有利于粗差发现等优势。作者以此为基础建立的稀少控制点SAR影像的几何纠正、立体定位以及区域网平差技术和方法，在中国西部1∶5万地形图空白区测图工程中一些常年云雾积雪覆盖的测区，也得到了很好的应用。理论和试验表明，本文改进的R-Cp构像模型和建立的R-Cp严密定位模型，有利于促进雷达遥感影像摄影测量数据处理理论和应用水平的提高。

参考文献(References)

程春泉, 张继贤, 邓喀中, 张力. 2012. 雷达影像几何构像距离-共面方程. 遥感学报, 16(1): 38–49

Cumming I G and Wong F H C. 2005. Digital Processing of Synthetic Aperture Radar Data: Algorithms and Implementation. Boston: Artech House, Inc

Dunn O J. 1959. Confidence intervals for the means of dependent, normally distributed variables. Journal of the American Statistical Association, 54(287): 613–621

France SPOT Image Company. 2002. SPOT Satellite Geometry Handbook, S-NT-73_12-SI, Edition 1, Revision 0. 15. 01. 2002

国家测绘局. 2010. 中华人民共和国测绘行业标准[CH/T 9009.3-2010]. 基础地理信息数字成果1:5000 1:10000 1:25000 1:50000 1:100000数字正射影像图. 3–3

Johnsen H, Lauknes L and Guneriussen T. 1995. Geocoding of fast-delivery ERS-1 SAR image mode product using DEM data. International Journal of Remote Sensing, 16(11): 1957–1968 [DOI: 10.1080/01431169508954532]

Konecny G and Schuhr W. 1988. Reliability of Radar Image Data. 16th ISPRS, (16): 92–101

Leberl F. 1978. Radargrammetry for Image Interpretation. ITC Technical Report

Leberl F W. 1990. Radar Grammetric Image Processing. Norwood: Artech House

单杰. 2002. 摄影测量与非摄影测量观测值的联合平差. 北京: 测绘出版社: 96–115

陶本藻. 2001. 自由网平差与变形分析. 武汉: 武汉测绘科技大学出版社: 1–77

王之卓. 1979. 摄影测量原理. 北京: 测绘出版社: 93–103

尤红建, 丁赤飚, 付琨. 2007. SAR图像对地定位的严密共线方程模型. 测绘学报, 36(2): 158–162

袁修孝. 2001. GPS辅助空中三角测量原理及应用. 北京: 测绘出版社: 57–62

袁修孝, 吴颖丹. 2010. 缺少控制点的星载SAR遥感影像对地目标定位. 武汉大学学报 (信息科学版), 35(1): 88–91

张力, 张继贤, 陈向阳, 安宏. 2009. 基于有理多项式模型RFM的稀少控制SPOT-5卫星影像区域网平差. 测绘学报, 38(4): 302–310

章仁为. 1998. 卫星轨道姿态动力学与控制. 北京: 北京航空航天大学出版社: 137